Spitsbergen Oceanic and Atmospheric interactions (SOA)

Manuel Bensi[1], Vedrana Kovačević[1], Leonardo Langone[2], Stefano Miserocchi[2], Maurizio Demarte[3], Roberta Ivaldi[3]

1 National Institute of Oceanography and Experimental Geophysics, Sgonico (Trieste), 34010, Italy
2 Institute of Polar Sciences, National Research Council of Italy, Via P. Gobetti 101, 40129 Bologna, Italy
3 Italian Navy Hydrographic Institute, Genova, 16126, Italy

Corresponding author: Manuel Bensi, mbensi@inogs.it, https://orcid.org/0000-0002-0548-7351

Keywords: Deep sea thermohaline variability, along slope currents, shelf-slope dynamics

1. Introduction

The Fram Strait is a crossroad of water masses that along its eastern part head towards the Arctic Ocean, and along its western edge, towards the Atlantic Ocean. This region is therefore strongly characterized by the interaction between waters of Atlantic and Arctic origins and by the local/remote atmospheric forcing and sea ice formation/melting, which contribute to driving the global thermohaline circulation (Skogseth et al. 2007; Nilsen et al. 2016; Onarheim and Årthun 2017; Polyakov et al. 2017; Bensi et al. 2019a). To understand the oceanic long-term

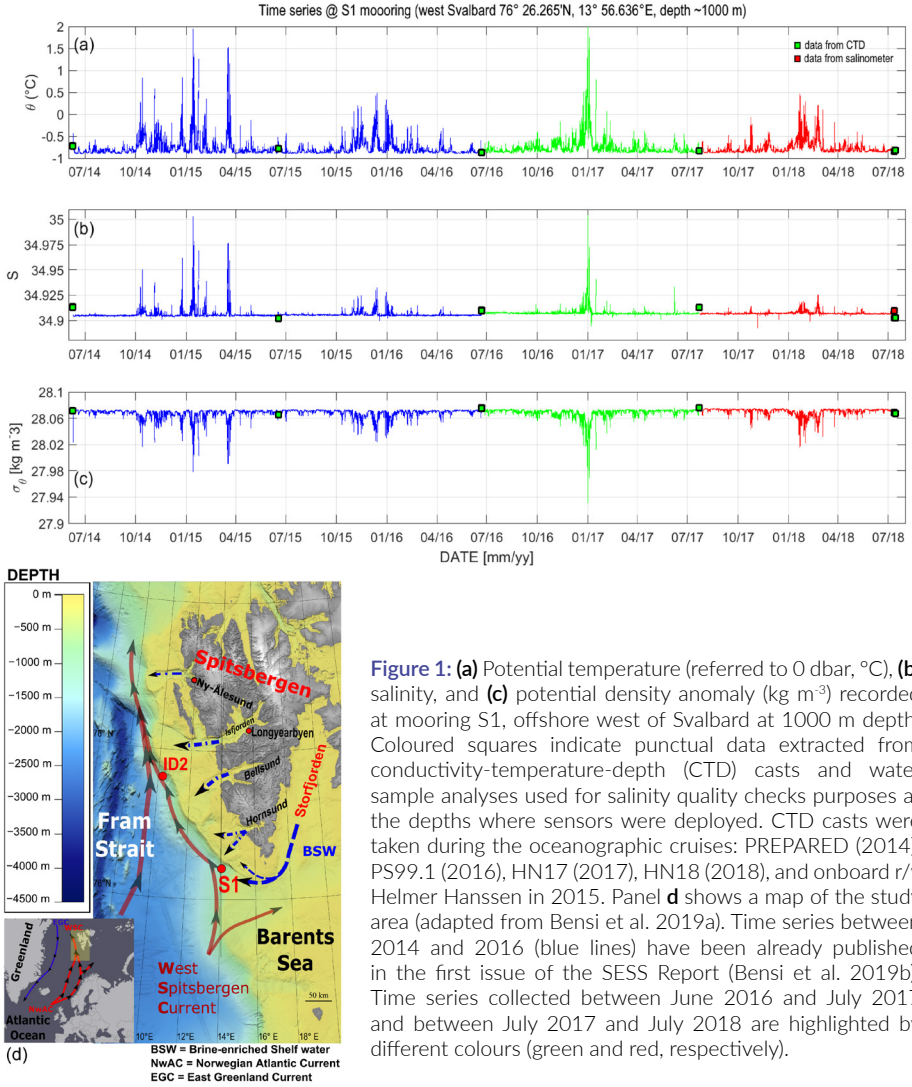

Figure 1: **(a)** Potential temperature (referred to 0 dbar, °C), **(b)** salinity, and **(c)** potential density anomaly (kg m^{-3}) recorded at mooring S1, offshore west of Svalbard at 1000 m depth. Coloured squares indicate punctual data extracted from conductivity-temperature-depth (CTD) casts and water sample analyses used for salinity quality checks purposes at the depths where sensors were deployed. CTD casts were taken during the oceanographic cruises: PREPARED (2014), PS99.1 (2016), HN17 (2017), HN18 (2018), and onboard r/v Helmer Hanssen in 2015. Panel **d** shows a map of the study area (adapted from Bensi et al. 2019a). Time series between 2014 and 2016 (blue lines) have been already published in the first issue of the SESS Report (Bensi et al. 2019b). Time series collected between June 2016 and July 2017 and between July 2017 and July 2018 are highlighted by different colours (green and red, respectively).

variability related both to natural and anthropogenic causes, especially in sensitive areas such as the Svalbard Archipelago, it is fundamental to collect long time series. At the same time, efficient monitoring and predicting of the world ocean must be a collaborative effort, useful to optimize and integrate ocean observing systems, sensors deployment and usage, and quality check of the data (Pearlman et al. 2019). Moreover, oceanographic data have to be analysed together with atmospheric ones, and with data collected on land, to provide a comprehensive view of the links between the different Earth's spheres. Here, we briefly present the updated time series collected by means of the deep-sea oceanographic mooring named S1, located south-west offshore Svalbard at ~1040 m depth (Lat. 76° 26.28'N Lon. 13° 56.91'E, Figure 1). Actually, the data series for temperature, salinity, dissolved oxygen, turbidity, and horizontal currents span over a time interval from June 2014 until July 2018. Data from June 2016 to July 2018 integrate those presented in the first issue of the SESS report released in January 2019 (Bensi et al. 2019b, data from 2014-2016). The comparison of oceanographic time series collected at S1 with atmospheric data (air temperature, wind speed and direction, heat fluxes at the air-ocean interface) provides information about the variability that characterizes the deep-sea layer along the West Svalbard continental margin (Bensi et al. 2019a). Atmospheric time series (air temperature, wind speed and direction, heat-fluxes at the air-ocean interface) are obtained from the ECMWF ERA-interim (European Centre for Medium-range Weather Forecasts) dataset.

2. The state of the oceanographic time series from mooring station S1 (76° N, 013° E)

Thermohaline data collected at S1, at depths between ~900 m and ~1000 m, reveal periodical peaks in temperature and salinity, which are translated into temporary reductions of the deep layer density, in particular between October and April. During 4 years of measurements, the most extreme episode was recorded between the end of 2016 and the beginning of 2017, when data showed that the potential temperature and salinity exceeded 2.5 °C and 35,

Table 1: Extreme values recorded at 1000m depth, at S1 mooring station, between October and April. Typical values of potential temperature, salinity, and potential density within the Norwegian Deep Sea Water at 1000 m depth in this region are -0.91 °C, 34.91, and 28.07 kg m^{-3}.

	Oct-Apr 2014-2015	Oct-Apr 2015-0216	Oct-Apr 2016-2017	Oct-Apr 2017-2018
Potential temperature (°C)	max 1.94	max 0.48	max 2.53	max 0.47
Salinity	max 35.00	max 34.97	max 35.00	max 34.92
Potential density anomaly (kg m^{-3})	min 27.978	min 28.02	min 27.93	min 28.01
Current magnitude (cm s^{-1})	max 60	max 35	max 85	max 49

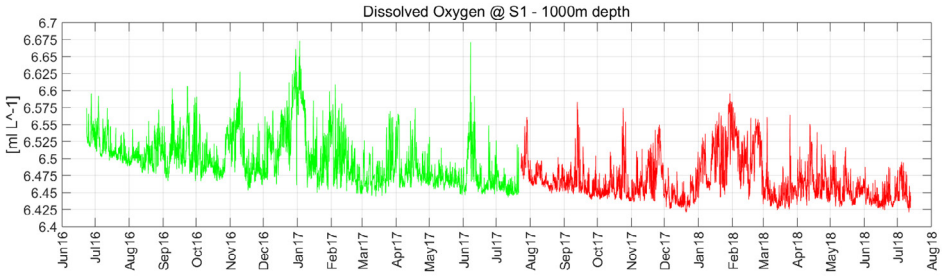

Figure 2: Dissolved oxygen (ml l^{-1}) recorded at S1. Data cover the period from June 2016 to July 2018. The optical sensor used was the Sea-Bird Electronics SBE 63, mounted on a SBE-37-ODO microcat. Time series collected between June 2016 and July 2017 and between July 2017 and July 2018 are highlighted by different colours (green and red, respectively).

respectively (Figure 1). Peak values of thermohaline properties and currents that occurred between 2014 and 2018 on the West Svalbard continental slope are reported in Table 1. Peaks in temperature and salinity were recorded in winters in which the maximum current speeds were also higher. The most extreme event, at the end of 2016 and the beginning of 2017, was indeed characterized by currents with magnitude up to 85 cm/s. The analysis of the direction revealed also an abrupt change from NW to SE, similarly to what was observed during other events within the period 2014-2016 (Bensi et al. 2019a). This change in flow direction followed a several-days period of enhanced temperature variations. From June 2016 onwards, dissolved oxygen concentrations were also recorded at S1. This parameter can provide information about the origin of the water that temporarily reaches a depth of 1000 m. In fact, higher values of dissolved oxygen are a signal that water intrusions belong to water masses that have been more or less recently in contact with the atmosphere. Apart from a slight negative trend that could be attributable to the instrumental drift of the sensor (Figure 2) we observed that peaks in temperature and salinity were accompanied, usually, by larger oxygen values. This fact suggests that water intrusions in the deep layer occupied by the Norwegian Deep Sea Water provide not only heat and salt, but also increased oxygenation. During the deployment phase between July 2017 and July 2018, 4 temperature sensors recorded data at different depths, spanning from 885 m to 1006 m (Figure 3). The time-depth diagram of temperature interpolated in the deep layer helps to better understand the origin and propagation of the warm water intrusions within this layer. We found that they occur about every 3-4 weeks. During the sub-period between January and March (Figure 3, lower panel), their occurrence increased, and the sensors recorded at least 5 episodes in which temperature peaks were close or above 1.5 °C. Individual episodes lasted about 10-24 hours, although sometimes they were included in longer events (lasting several days) that characterized a general increase in temperature in the deep layers. Temperature peaks usually were higher in the upper part of the bottom layer, and sometimes they did not reach the deepest sensors (see e.g. episodes in October 2017 and on 1-2 March 2018), proving that the warm water intrusions are connected with the water masses from the layer above.

2.1 Periodic oscillations and low-frequency variability

During the investigated time interval (2016-2018) the mooring station S1 was also equipped with a pressure sensor, positioned at ~ 40 m from the sea bed (at depth of ~ 1004 m), which showed large-amplitude periodic oscillations (Figure 4). Statistical and harmonic analysis techniques applied to the data provided information about the tidal signal. Moreover, de-tided bottom pressure time series are able to reveal oscillations of the water column

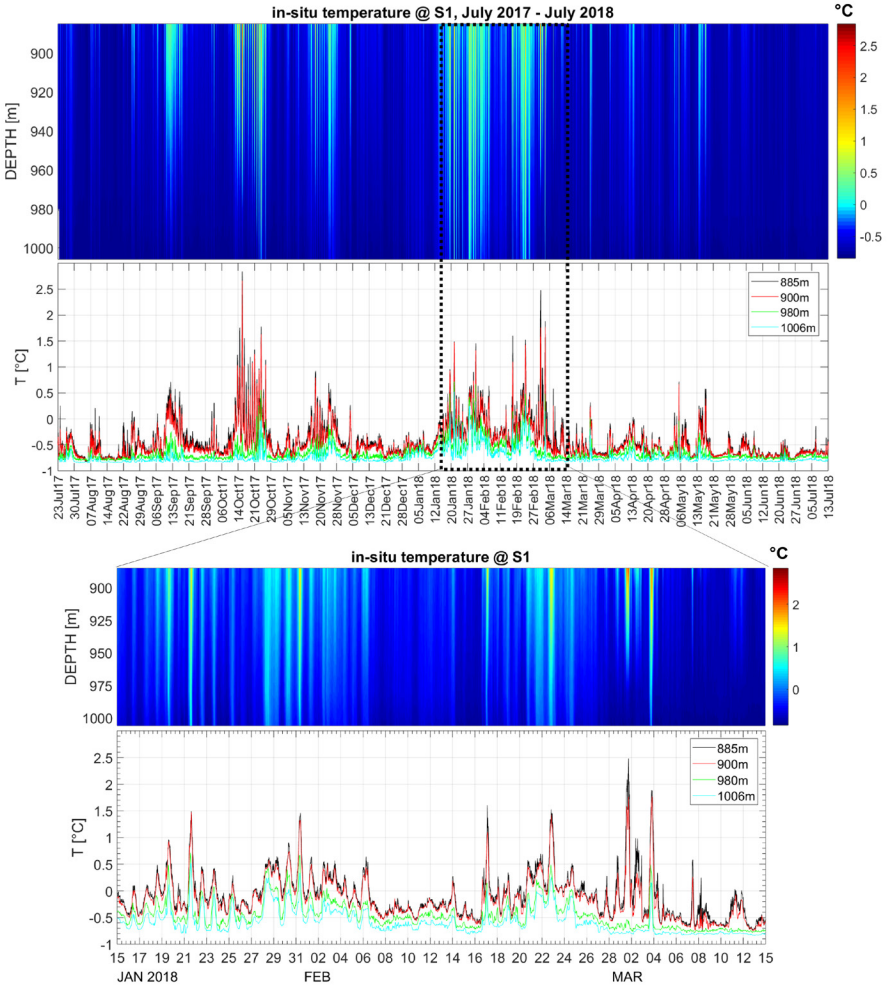

Figure 3: Time series of *in situ* temperature (°C) collected at different depths at S1 mooring station, between July 2017 and July 2018. The lower panel shows the same data with a zoom on the period 15 Jan - 15 Mar 2018.

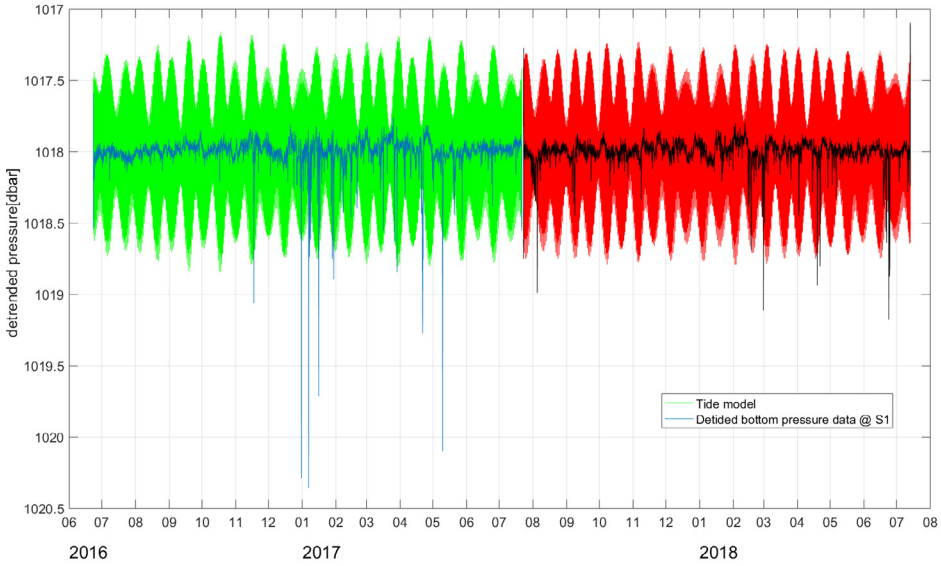

Figure 4: Tidal records (green and red refers to the two deployment phases) and residual bottom pressure time series (blue and black) obtained at S1 mooring station, offshore west of Svalbard at 1000 m depth between June 2016 and July 2017.

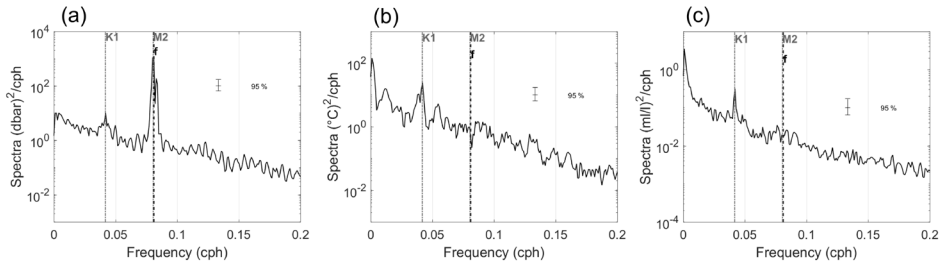

Figure 5: Spectral analysis of June 2016 - July 2017 hourly time series: raw pressure (a), potential temperature (b), dissolved oxygen concentration (c). Spectra of salinity and potential density anomaly are quite similar to those of the potential temperature, and therefore not shown. The spectra referred to the period 2017-2018 are alike. K1 (period 23.94 h) and M2 (12.42 h) are the most typical representatives of the diurnal and semidiurnal tidal constituents, respectively, while f is the inertial frequency at the latitude of S1 (period 12.34 h).

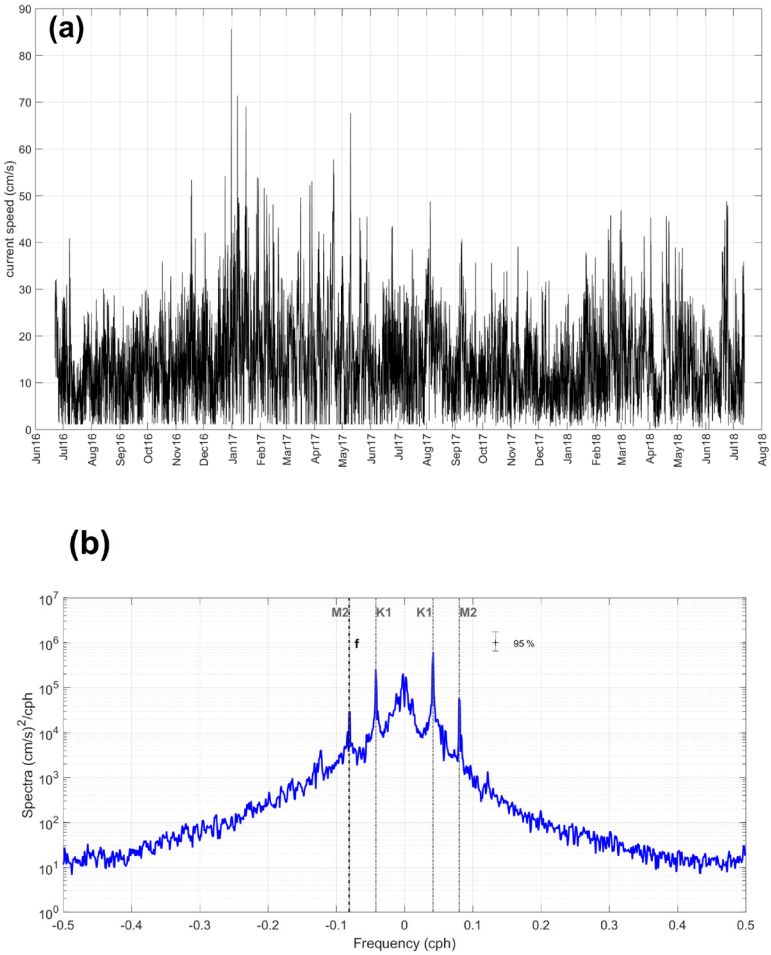

Figure 6: (a) Time series of the current speed (cm s^{-1}) at S1 (1000m depth) in the period June 2016 - July 2017**. (b)** The rotary spectrum of u (eastward) and v (northward) components of the same current time series (negative/positive frequencies refer to anticyclonic/cyclonic rotations). The power spectrum of the same dataset from July 2017 - July 2018 has very similar characteristics.

that are not related to the tides, and hence can be associated with other signals. The power spectrum analysis has been performed separately for each yearly deployment period due to the time gap between the mooring recovery and re-deployment. Both periods confirm that the large-amplitude diurnal and semidiurnal oscillations are due to the tidal movements of the sea level (corresponding to about 1 m amplitude). The variance due to these oscillations is far more important than any other periodic signals of the pressure and the semidiurnal is more energetic than the diurnal one (Figure 5a). The low-frequency part is emerging only in

the residual pressure values (tidal constituents filtered out). Oscillations of the thermohaline properties, as shown for the potential temperature (Figure 5b), and dissolved oxygen (Figure 5c) seem to be significantly energetic at the low-frequency spectrum end (i.e., at periods of about 3-4 days and about 40 days). Tidal peaks are also evident, but the diurnal one is more energetic than the semi-diurnal, contrary to that of the pressure. The significant oscillations of the turbidity at 1000 m depth are concerning the low-frequency band, and there are only some correspondences with the already evident tidal bands (not shown). Note also that turbidity during 2016-2017 refers to the 900 m depth (140 m above the sea bed). Its power spectrum (not shown) has no significant oscillations at that depth, except at the very low-frequency spectrum end. We believe that the different depth at which the turbidity sensor was placed during 2016-2017 (900 m) and 2017-2018 (1000 m) can explain the slightly higher energy both at the diurnal and long-period time scales found during the second year of measurements. This behaviour could be partially related to the fact that some periodic turbidity oscillations are mostly driven by a sediment resuspension from the sea bed, while the occasional significant turbidity increase, often unlinked with the thermohaline parameters, is related possibly to another kind of phenomena, e.g. the advection of the sediment-rich near-bottom flow from slope/shelf areas. The deep horizontal currents appeared also influenced by the diurnal and semidiurnal signals, as well as by the low-frequency fluctuations (with periods of about 3 weeks, Figure 6). The rotations in the positive sense (cyclonic) were slightly more energetic than in the negative (anti-cyclonic) sense and diurnal oscillations have more variance than the semidiurnal ones. The particularity of the semidiurnal band of the current flow is the overlapping of the semidiurnal tidal and inertial frequencies, the latter being present in marine currents, and absent in the sea-level (pressure). The only ECMWF atmospheric variables showing the diurnal, although rather weak, signal are air temperature at 2 m height and to a lesser extent, the mean sea level air pressure. Wind components are oscillating energetically only at long periods, from a week onward (not shown).

2.2 Concluding remarks

As observed during four years (2014-2018) of thermohaline and current recordings, the deep layer at the West Svalbard slope was perturbed several times with peculiar manifestations of thermohaline properties, currents, and turbidity, as noticed above and in Bensi et al. (2019a, b). Not all the phenomena occurred simultaneously, and often turbidity variations were decoupled from the thermohaline variability. As an example of such events we took those from the period December 2016 - January 2017, when the amplitudes of variability were particularly large concerning temperature and currents. An exceptional increase in temperature, changing its sign from negative to positive, was reflected in simultaneous salinity increase, and density decrease. Each of such events lasted about 10 days (one in the period December - January 2016-2017 and two in the period January -

February 2018). There was no concomitant significant increase of turbidity, which, instead, increased significantly during a similar event occurred at the beginning of March 2018 at the depth of about 1000 m. The current field appeared quite uniform during such events, and NW direction was almost unperturbed, except for the daily oscillations, manifesting as cycloidal motions. However, as these events ceased, and the temperature returned to the usual level (-0.9 °C), the current flow reversed for about several days (e.g. two weeks after the event recorded at the end of 2016), before resuming its prevalent NW direction.

Synergies with other SESS report chapters: in the SESS Report 2018 the SOA chapter (Bensi et al. 2019b) included considerations on the relation between atmospheric processes (wind data) and the dynamic response of the deep sea west of Svalbard. Here we foresee a potential for greater interaction among scientists working on different research topics to discuss important aspects such as: the carbonate system and the CO_2 uptake from the land and ocean (e.g. link with chapters in this report on "Atmospheric black Carbon at Svalbard" (Gilardoni et al. 2020) and "Mapping of plant productivity" (Karlsen et al. 2020), and the effects of melt water runoff from fjords on the offshore marine system (e.g. link with chapters on "The state of Svalbard glaciers" (Schuler et al. 2020) and "Atlantification of Svalbard fjords" (Cottier et al., 2019).

3. Unanswered questions

How do internal dynamics influence the mixing rate between upper and deep layers along the West Spitsbergen continental slope, contributing to the slow modification of the deep layer (> 800 m depth) in this Arctic region?

What is the long-term effect of these continuous intrusions of warmer and saltier water into the deep layers of the Fram Strait? Will they, in turn, have an effect on the progressive warming of the Arctic Ocean?

Can numerical models help resolve the processes observed experimentally in the deep sea west of Svalbard, and help predicting long-term changes possibly induced by them?

4. Recommendations for the future

The *integration of in situ data (fixed ocean and land stations, hydrographic cruises) with other data collection platforms, such as ARGO floats*[1] *and high-resolution satellite images would ensure a better interpretation of the oceanographic phenomena, especially the extreme ones*. In addition, the Synthetic-aperture radar (SAR) satellite images, which are not affected by the cloud cover, could be used for the analysis of wind, waves, and the sea ice cover variability.

Output from high-resolution numerical models could be used to better interpret the dynamic response of the deep ocean to changes in atmospheric pressure, and thus to study the generation and propagation of internal topographically trapped waves.

Set up access programmes to marine infrastructure open to third parties as well, with the aim of guaranteeing implementation and maintenance of the offshore observational sites, to achieve time series useful for climatic considerations. SIOS could extend the call for access to infrastructure including marine sites (within fjords and offshore), and providing the necessary logistic support to access such infrastructures. This would ensure greater visibility of the data, greater collaboration, and optimisation of the existing infrastructure. A specific example could be the possibility, through transnational access calls, to add biogeochemical sensors and/or more levels of turbidity sensors at mooring station S1. This approach would also ensure greater interaction between coastal (fjords) and offshore studies (e.g., concerning carbonate system, organic and inorganic outflow from fjords).

A programme of harmonisation of marine measurements around Svalbard would be desirable in the near future in order to ensure homogeneous data collection in different areas. *A medium-term objective could be to create a handbook of best practices applicable to the measurements carried out around the archipelago.*

1 http://www.argo.ucsd.edu

5. Data availability

Table 2 summarizes the datasets used and presented in this SESS report card.

Table 2: Dataset presented in the SESS report chapter SOA

Parameter (time series) [depth ~ 1000 m; *Latitude: 76° 26.28' N; Longitude: 013° 56.91' E*	Period covered	Data provider	Metadata/Data access
Temperature/Salinity	June 2014 - July 2018	OGS/ISP	NODC (OGS)/Seadatanet/ Data will be available through the SIOS data access point
Turbidity	June 2014 - July 2018	OGS/ISP	NODC (OGS)/Seadatanet/ Data will be available through the SIOS data access point
Dissolved Oxygen	June 2016 - July 2018	OGS/ISP	NODC (OGS)/Seadatanet/ Data will be available through the SIOS data access point
Horizontal currents (u, v)	June 2014 - July 2018	OGS/ISP	NODC (OGS)/Seadatanet/ Data will be available through the SIOS data access point

Acknowledgements

We thank the Captains and crew (scientific and technical) of the research vessel Alliance during High-North cruises (The 'High North' programme is managed by the Italian Navy Hydrographic Institute). We appreciate SIOS-KC staff for their continuous effort spent in promoting research and outreach activities in Svalbard. This work was supported by the Research Council of Norway, project number 251658, Svalbard Integrated Arctic Earth Observing System - Knowledge Centre (SIOS-KC).

References

Bensi M, Kovačević V, Langone L, et al. (2019a) Deep Flow Variability Offshore South-West Svalbard (Fram Strait). Water 11:683. https://doi.org/10.3390/w11040683

Bensi M, Kovačević V, Ursella L, Rebesco M, Langone L, Viola A, Mazzola M, Beszczyńska-Möller A, Goszczko I, Soltwedel T, Skogseth R, Nilsen F, Wåhlin A (2019b) Spitsbergen Oceanic and Atmospheric interactions -SOA. In: Orr et al. (eds): SESS report 2018, Svalbard Integrated Arctic Earth Observing System, Longyearbyen, pp. 130-146. https://sios-svalbard.org/SESS_Issue1

Cottier F, Skogseth R, David D, Berge J (2019) Temperature time-series in Svalbard fjords. A contribution from the "Integrated Marine Observatory Partnership". In: Orr et al. (eds): SESS report 2018, Svalbard Integrated Arctic Earth Observing System, Longyearbyen, pp. 108-118. https://sios-svalbard.org/SESS_Issue1

Gilardoni S, Lupi A, Mazzola M, Cappelletti DM, Moroni B, Ferrero L, Markuszewski P, Rozwadowska A, Krejci R, ZiegerP, Tunved P, Karlsson L, Vratolis S, Eleftheriadis K (2020) Atmospheric Black Carbon in Svalbard. In: Van den Heuvel et al. (eds): SESS report 2019, Svalbard Integrated Arctic Earth Observing System, Longyearbyen, 196 - 211 . https://sios-svalbard.org/SESS_Issue2

Karlsen SR, Stendari L, Nilsen L, Malnes E, Eklundh L, Julitta T, Burkhart A, Tømmervik H (2020) Sentinel based mapping of plant productivity in relation to snow duration and time of green-up. In: Van den Heuvel et al. (eds): SESS report 2019, Svalbard Integrated Arctic Earth Observing System, Longyearbyen, 42 - 57 . https://sios-svalbard.org/SESS_Issue2

Nilsen F, Skogseth R, Vaardal-Lunde J, Inall M (2016) A Simple Shelf Circulation Model: Intrusion of Atlantic Water on the West Spitsbergen Shelf. J Phys Oceanogr 46:1209–1230. https://doi.org/10.1175/JPO-D-15-0058.1

Onarheim IH, Årthun M (2017) Toward an ice-free Barents Sea. Geophys Res Lett 44:8387–8395. https://doi.org/10.1002/2017GL074304

Pearlman J, Bushnell M, Coppola L, et al. (2019) Evolving and Sustaining Ocean Best Practices and Standards for the Next Decade. Front Mar Sci 6. https://doi.org/10.3389/fmars.2019.00277

Polyakov IV, Pnyushkov AV, Alkire MB, et al. (2017) Greater role for Atlantic inflows on sea-ice loss in the Eurasian Basin of the Arctic Ocean. Science 356:285–291. https://doi.org/10.1126/science.aai8204

Schuler TV, Glazovsky A, Hagen JO, Hodson A, Jania J, Kääb A, Kohler J, Luks B, Malecki J, Moholdt G, Pohjola V, van Pelt W (2020), SvalGlac: New data, new techniques and new challenges for updating the state of Svalbard glaciers. In: Van den Heuvel et al. (eds): SESS report 2019, Svalbard Integrated Arctic Earth Observing System, Longyearbyen, 108 - 135 . https://sios-svalbard.org/SESS_Issue2

Skogseth R, Sandvik AD, Asplin L (2007) Wind and tidal forcing on the meso-scale circulation in Storfjorden, Svalbard. Cont Shelf Res 27:208–227. https://doi.org/10.1016/j.csr.2006.10.001